

Article

Nanocarbon-Based Mixed Matrix Pebax-1657 Flat Sheet Membranes for CO₂/CH₄ Separation

Athanasios N. Vasileiou^{1,2,†}, George V. Theodorakopoulos^{1,2,*,†}, Dionysios S. Karousos¹, Mirtat Bouroushian², Andreas A. Sapalidis¹ and Evangelos P. Favvas^{1,*}

¹ Institute of Nanoscience and Nanotechnology, National Center for Scientific Research “Demokritos”, Aghia Paraskevi, 15341 Attica, Greece; purinikos@hotmail.com (A.N.V.); d.karousos@inn.demokritos.gr (D.S.K.); a.sapalidis@inn.demokritos.gr (A.A.S.)

² School of Chemical Engineering, National Technical University of Athens, 9 Iroon Polytechniou Street, Zografou, 15780 Athens, Greece; mirtatb@central.ntua.gr

* Correspondence: g.theodorakopoulos@inn.demokritos.gr (G.V.T.); e.favvas@inn.demokritos.gr (E.P.F.)

† These authors contributed equally to this work.

Abstract: In the present work, Pebax-1657, a commercial multiblock copolymer (poly(ether-block-amide)), consisting of 40% rigid amide (PA6) groups and 60% flexible ether (PEO) linkages, was selected as the base polymer for preparing dense flat sheet mixed matrix membranes (MMMs) using the solution casting method. Carbon nanofillers, specifically, raw and treated (plasma and oxidized) multi-walled carbon nanotubes (MWCNTs) and graphene nanoplatelets (GNPs) were incorporated into the polymeric matrix in order to improve the gas-separation performance and polymer’s structural properties. The developed membranes were characterized by means of SEM and FTIR, and their mechanical properties were also evaluated. Well-established models were employed in order to compare the experimental data with theoretical calculations concerning the tensile properties of MMMs. Most remarkably, the tensile strength of the mixed matrix membrane with oxidized GNPs was enhanced by 55.3% compared to the pure polymeric membrane, and its tensile modulus increased 3.2 times compared to the neat one. In addition, the effect of nanofiller type, structure and amount to real binary CO₂/CH₄ (10/90 vol.%) mixture separation performance was evaluated under elevated pressure conditions. A maximum CO₂/CH₄ separation factor of 21.9 was reached with CO₂ permeability of 384 Barrer. Overall, MMMs exhibited enhanced gas permeabilities (up to fivefold values) without sacrificing gas selectivity compared to the corresponding pure polymeric membrane.

Keywords: mixed matrix membranes (MMMs); supported thin films; carbon nanofillers; Pebax-1657; CNTs dispersion; GNPs dispersion; gas separation



Citation: Vasileiou, A.N.; Theodorakopoulos, G.V.; Karousos, D.S.; Bouroushian, M.; Sapalidis, A.A.; Favvas, E.P. Nanocarbon-Based Mixed Matrix Pebax-1657 Flat Sheet Membranes for CO₂/CH₄ Separation. *Membranes* **2023**, *13*, 470. <https://doi.org/10.3390/membranes13050470>

Academic Editor: Juliana Isabel Clodt

Received: 4 April 2023
Revised: 24 April 2023
Accepted: 26 April 2023
Published: 28 April 2023



Copyright: © 2023 by the authors. Licensee MDPI, Basel, Switzerland. This article is an open access article distributed under the terms and conditions of the Creative Commons Attribution (CC BY) license (<https://creativecommons.org/licenses/by/4.0/>).

1. Introduction

In recent years, gas separation, such as N₂ production, H₂ recovery, CO₂ capture and natural gas sweetening, is achieved with polymeric membranes, an efficient process competing sufficiently with well-established separation processes such as adsorption, extraction and cryogenic distillation [1]. Membranes offer easy fabrication and scalability, low capital and operating cost, operation simplicity, low energy consumption and maintenance, mechanical reliability and small carbon footprint. All these features render them a promising method in high-performance gas-separation applications [2]. However, the gas-separation performance of polymeric membranes is frequently restricted by the Robeson’s trade-off upper bound [3]. Polymers with high permeability exhibit low selectivity and vice versa [3,4].

To address this, nanotechnology is used in membrane science, creating a new type of nanoengineered materials, where the membrane properties are modified in the direction of improving the filtration/separation processes [5]. Among numerous different modification

processes, such as polymer blending [6], cross-linking [7], surface modification [8], surfactant/salt addition [9,10], high-energy x-ray irradiation [11], thermal treatment, annealing post-treatment [12] and immobilization of specific ligands [13], the preparation of mixed matrix membranes, by adding functional nanomaterials into polymer matrix, is a promising technique for the preparation of membranes with improved separation properties [14].

Hence, nanoporous carbon-based nanofillers are incorporated into polymer matrices as a dispersed phase forming mixed matrix membranes (MMMs), which subsequently can provide an increase in selectivity and permeability simultaneously [15]. This fact makes them promising types of filler material in high-performance gas-separation applications [2,15,16] by combining the gas-separation properties of inorganic, e.g., molecular sieve, particles with the advantageous properties of a polymeric matrix [17]. However, MMMs still present shortcomings such as physical aging, plasticization and also low processing capacity [18]. Criteria for the selection of membrane materials, both for polymer matrices and added fillers, are key and significant parameters of preparing highly selective, highly permeable and overall efficient membranes [19]. A crucial factor for this selection is the requested separation, which we are interested in working on. For example, in the case of CO₂/CH₄ separation, a criterion for polymeric material selection is the existence of a high affinity to polar molecules, such as CO₂, compared to nonpolar molecules, such as CH₄. The requirements for good mechanical behavior and of course high resistance to thermal and chemical strains also remain. Among many other polymeric membrane materials, such as polysulfones, polyimides, polyamides, polyesters and cellulose acetate, poly(ether-block-amide) (Pebax) is classified as one material which satisfies adequately the abovementioned requirements [20,21]. Based on the fact that one of the approaches for overcoming the undesirable trade-off relationship between permeability and selectivity is to use polymeric materials, which combine the flexibility of polymers such as polyethers (PEs) and the stability of rigid polymers such as polyamides (PAs), polyether block amide copolymers (PEBAs) are classified as some of the most promising materials for CO₂ selective membrane fabrication [22]. The PE segment in the polymer structure is responsible for permeability of penetrants through the membrane owing to high mobility of chains in the polymer matrix, whereas the PA segment is impermeable [21].

The prospects offered by this material's family have attracted the interest of many research groups worldwide, and during the last two decades many encouraging studies have been conducted based on Pebax gas-selective membranes in literature. Some relevant works and their main evidence in chronological order are reported in the following.

Liu et al. [23], in 2014, prepared and studied a series of hydrogel membranes from chitosan (CS)/polyether-block-amide (Pebax) blends. These membranes exhibited high CO₂ permeabilities along with good operation stabilities. Specifically, the membrane with a mass ratio of CS to Pebax equal to 1:1 showed a very high CO₂ permeability of about 2880 Barrer and a CO₂/CH₄ separation factor of ~23 at 85 °C. The gas permeability/selectivity experiments were performed in the presence of relative humidity >98%, which facilitated transport membrane separation. Estahbanati et al. [24], in 2017, incorporated features of the Pebax-1657 copolymer by adding [BMIM][BF₄] ionic liquid to increase the permselectivity of the membranes for CO₂/light gas separation, because the CO₂ solubility in ionic liquids (ILs) increases with pressure increment and temperature decrement. In addition, due to the high affinity of CO₂ in both polymer and IL, both CO₂ permeability and selectivity increased simultaneously with increasing IL content. Their hypothesis was confirmed by gas permeation results, where at 35 °C and 10 bar, the CO₂ permeability increased from 110 Barrer for neat Pebax to 190 Barrer in the blended membrane containing 50 wt.% IL. The corresponding CO₂/CH₄ and CO₂/N₂ selectivities increased from 20.8 to 24.4 (about 17%) and from 78.6 to 105.6 (about 34%), respectively.

Zhang et al. [25], in 2018, reported that by microphase separation the polymer chain packing density changes along with the molecular separation efficiency within the composite halloysite nanotube (HNT)/Pebax-1657 membranes. This fact was taken into consideration in the case of a thin composite Pebax membrane, through the controllable self-assembly

of one-dimensional halloysite nanotubes (HNTs, up to 0.2 wt.% towards the casting solution) within the thin film via a solution casting technique. This change in crystallization of the polyamide component, which was induced at the HNT surface, provided the composite membrane an ultrahigh CO₂/N₂ selectivity of up to 290 combined with a moderate CO₂ permeability of 80.4 Barrer. In another work, in 2019, Farashi et al. [21] studied Pebax-1657 mixed matrix membranes by using different contents of aluminum oxide (Al₂O₃) (0, 2, 4, 6 and 8 wt.%) in the polymer matrix (Pebax). Permeances of pure CO₂ and CH₄ gases were measured in the range of pressures between 3 and 15 bar at 25 °C. The results revealed better separation efficiency (both CO₂ permeability and CO₂/CH₄ selectivity) of the nanocomposite membranes than the pristine membrane. For example, the CO₂ permeability and ideal CO₂/CH₄ selectivity values for the neat membrane at the pressure of 3 bar were 123.46 Barrer and 21.21, respectively, whereas those values for the membrane comprising 8 wt.% of Al₂O₃ were 159.27 Barrer and 24.73, respectively.

In addition to the polymer matrix selection, the selection of the specific kind of filler membrane materials is another route for improving the selectivity performance of the membrane. Carbon-based nanomaterials are reported as promising filler materials for producing improved mixed matrix membranes for gas-separation applications [5]. Among others, multi-walled carbon nanotubes (MWCNTs) and graphene nanoplatelets (GNPs) [26,27] are two types of nanocarbons, nanoscale carbon derivative materials, which can provide the requested improvement of both permeability and selectivity performance of the derivative mixed matrix membrane if they are used as membrane filler materials. The fact that both MWCNTs and GNPs are relatively cheap and easily available materials combined with their good physicochemical properties have rendered them particularly popular in composite membrane technology. Among others, some of the advantages of these two nanomaterials are (1) the facile production methods, (2) the ability for surface modification using wet chemistry, (3) their dispersibility using sonication, (4) their conductive properties and (5) their large specific surface areas [28].

In current work, Pebax-MH1657, a commercial multiblock copolymer (poly(ether-block-amide)) with remarkable CO₂ separation properties was selected as the base polymer of MMMs. In addition, both raw and treated MWCNTs and GNPs were used as membrane filler materials for producing composite membranes of 0.7, 3.0 and 5.3 wt.% in carbon nanofillers relative to the polymer content. The characterization and the performance-evaluation of thirteen produced membranes were carried out by means of SEM, FTIR, gas mixture permeability evaluation for CO₂/CH₄ (10/90), contact angle measurements and mechanical tests.

2. Materials and Methods

2.1. Materials

Pebax MH 1657 (containing approximately 60 wt.% polyether segments and 40 wt.% polyamide segments) was purchased from Arkema S.A., France. Ethanol was purchased from VWR International Ltd., Lutterworth, UK. All of the above chemicals were of analytical grade and were used without further purification. Ultrapure water (Milli-Q, 18 MΩ·cm) was used throughout this study. The carbon nanofillers were provided from our colleagues from FutureCarbon GmbH, Bayreuth, Germany.

For the preparation of flat sheet Pebax-1657-based mixed matrix membranes, a dispersion of raw and treated (plasma or oxidized) multi-walled carbon nanotubes (MWCNTs) and graphene nanoplatelets (GNPs) was incorporated into the polymeric matrix in order to improve the gas-separation performance and the polymer's structural properties.

The raw GNPs were produced by a water-based milling process and for the wet chemical treatment of GNPs, KMnO₄ was employed as oxidizing agent. In addition, the raw MWCNTs were produced by chemical vapor deposition of hydrocarbon gas on iron-based catalysts, and for the functionalization of MWCNTs, plasma treatment was implemented (optimum operational parameters: He with 500 W plasma power for 10 min exposure time and O₂ with 500 W for 70 min exposure time).

Dispersions of all twelve different MMM systems were formed by the solution blending method with an additional dispersion step to avoid agglomeration. The obtained homogeneous solutions were poured into Petri dishes, and solvent evaporation was performed under controlled atmospheric conditions. Finally, the films were dried in an oven at 60 °C for 2 h in order to remove any residual solvent. The overall membrane preparation process is illustrated in Figure 1.

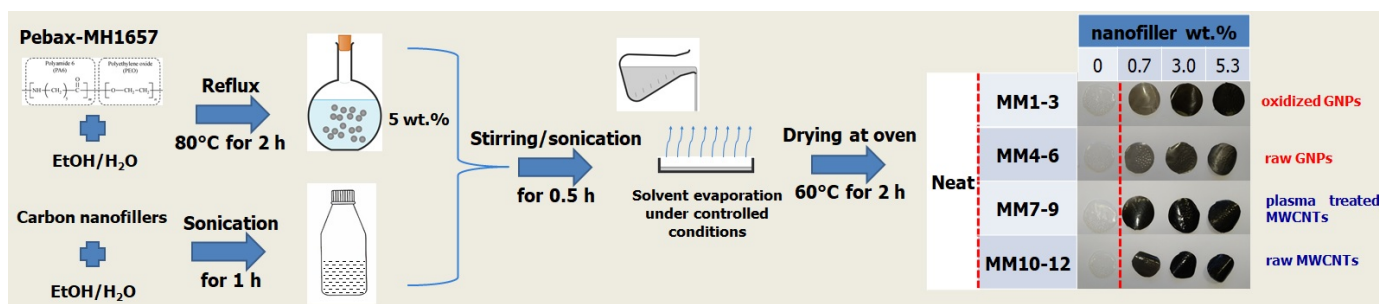


Figure 1. Schematic representation of all intermediate steps for Pebax-1657-based MMM production.

The status of dispersion quality was evaluated directly by optical determination of the solutions and the prepared membranes, as well as indirectly mainly by mechanical strength testing and microscopic analysis. After preparation, the membranes were dried, and permeation properties were analyzed for CO₂ and CH₄.

2.2. Instrumentation-Characterization

The composite carbon-based Pebax-1657 membranes were evaluated concerning their CO₂/CH₄ selectivity and permeability performance in a flow selectivity apparatus in conjunction with high-sensitivity gas chromatography. In addition, the prepared membranes were characterized by Fourier transform infrared spectroscopy (FTIR) conducted on a Nicolet Magna-IR Spectrometer 550 (Thermo Fisher Scientific, Waltham, MA, USA). The morphological characterization of selected samples was investigated by scanning electron microscopy (SEM) in a JEOL JSM-7401F instrument (Tokyo, Japan). The membranes' mechanical properties (Young's modulus, ultimate tensile strength and tensile elongation) were determined in a Thümler GmbH Tensile Tester Model (Roth, Germany) equipped with a PA6110 Nordic Transducer load cell with a maximum force of 250 N [29]. The specimens were prepared according to ASTM D882. Dynamic contact angle (CA) measurements of water/membrane interfaces took place using the Krüss DSA30S optical contact angle measuring instrument (Krüss GmbH, Hamburg, Germany).

2.3. Membrane Preparation

The first step of the membrane preparation process was the blending of the two solutions, "A" and "B". The "A" solution was prepared after solving the Pebax-MH1657 pellets, 5 wt.%, into EtOH/H₂O (70/30 wt.%) solvent, whereas the "B" solution was derived by dispersing the carbon nanofiller into the same solvent (EtOH/H₂O, 70/30 wt.%). The solution "A" was first refluxed at 80 °C for 2 h, and solution "B" was sonicated for 1 h. The final solution obtained after the mixing of both prepared solutions was stirred and sonicated for half an hour before it was poured into a flat glass Petri dish. Subsequently, the solvent was evaporated overnight at room temperature, and finally the films were dried in an electrical oven at 60 °C for a period of time of about two hours. In Table 1, all the studied cases for the MMMs preparation are presented.

Table 1. Concentrations of precursor solutions, polymer and carbon nanomaterials (CNMs) and final membrane concentrations after drying for the three studied cases of filler content.

Case	Polymer in Solution A	Filler in Solution B	Concentration in Final Solutions (A + B)		Filler Concentrations in MMMs
			Polymer	Filler	
“I”	5	0.052	3.0	0.021	0.7
“II”	5	0.225	3.0	0.090	3.0
“III”	5	0.398	3.0	0.159	5.3

All percentages in wt.%.

2.4. Gas Permeability/Separation Measurements under Continuous Flow Conditions

Gas permeability and selectivity evaluation was performed by the “flow method” using the gas chromatography (GC) technique. The gas permeance values were measured in the apparatus presented in Figure 2, where the permeate stream was directed to a highly sensitive gas chromatography instrument, and the permeance coefficient was calculated by the integration of the recorded GC peak [30]. As a carrier gas, helium was used (Figure 2). The experimental setup for the permeance measurements, using gas chromatography analysis, has been described in detail previously [31]. Using this setup, mixture selectivity experiments of 10/90 (mole concentration) for CO₂/CH₄ were performed.

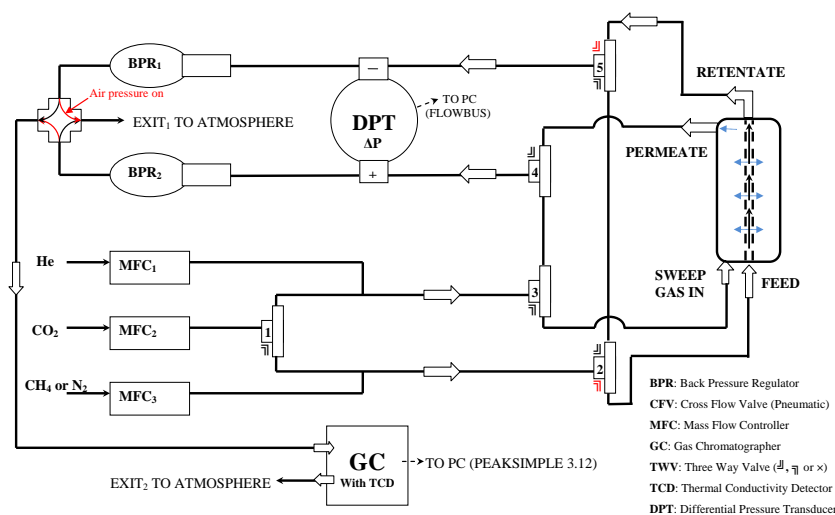


Figure 2. Scheme of laboratory apparatus for gas-separation experiments under continuous flow [32].

All thirteen flat sheet membranes, each one with an effective permeation area of about 5.3 cm², were successively inserted into a metallic (bronze) membrane housing. Each membrane was placed into the cell and thoroughly degassed for at least 24 h at 10^{−6} mbar and 80 °C before permeance/selectivity measurements.

The 10/90 CO₂/CH₄ (mole concentration) gas mixture was introduced to the feed side of the membrane, whereas helium was used as the sweep gas on permeate side. Mass flow controllers (Brooks Instruments 0–50 mL/min) were used to define the flow rates of each gas. In the retentate side, the pressure was controlled by a backpressure regulator, while the permeate side was maintained at atmospheric pressure. Transmembrane pressure was recorded using a differential manometer. An 8610C gas chromatograph equipped with high-sensitivity TCD and FID detectors was used for analysis of both gas lines.

The selectivity coefficients were calculated according to the following equation [33]:

$$S = \frac{A_{(gas1/permeate)} / A_{(gas2/permeate)}}{A_{(gas1/feed)} / A_{(gas2/feed)}} \tag{1}$$

where $A_{(gas1/permeate)}$, $A_{(gas1/feed)}$ and $A_{(gas2/permeate)}$, $A_{(gas2/feed)}$ are the peak surfaces for the permeate and feed gas streams, respectively.

3. Results and Discussion

3.1. Morphology of Nanofillers/Prepared MMMs

High-purity carbon nanotubes were produced by catalyst-assisted chemical vapor deposition [34] and were treated as described in Section 2.1. The GNPs were produced following the water-based milling process [35] and were oxidized using KMnO_4 as oxidizing agent (see Section 2.1). In the following Figure 3, SEM micrographs illustrate the morphology of MWCNTs and their interwoven and entangled arrangement. They appeared in the form of ribbon complexes with no sign of any impurities, and their outer diameter ranged between 13 and 23 nm. The GNPs fillers have a wide range of dimensions both in thickness and lateral dimensions, which fluctuate from 2 to 5 μm and from 50 to 100 nm, respectively. In addition, GNPs have a high purity and well-defined structure of uniform flakes.

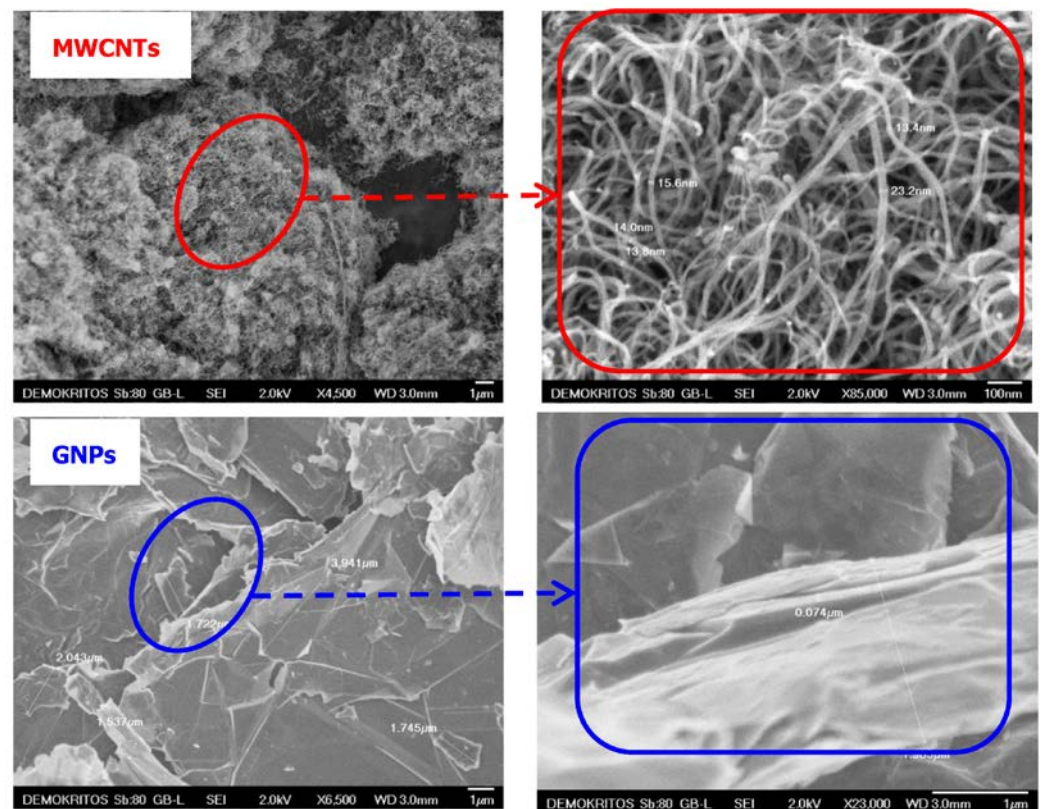


Figure 3. SEM images of raw multi-walled carbon nanotubes (MWCNTs) and graphene nanoplatelets (GNPs).

Figure 4 summarizes the SEM micrographs of four selected membranes. The selected membranes are the neat Pebax-MH1657 membrane, the MM5 sample (3 wt.% of raw GNPs relative to polymer content), the MM8 sample (3 wt.% of plasma-treated MWCNTs) and the MM11 sample (3 wt.% of raw MWCNTs). SEM images illustrate two main characteristics of the prepared membranes, namely that they show dense structure without any pinholes and that their thickness ranges from about 8 to 90 μm . Both carbon nanotubes and GNPs are not visible in the cross-sectional images of the three selected mixed matrix membranes in the presented range of magnitude, in which no significant differences in the matrix are observed.

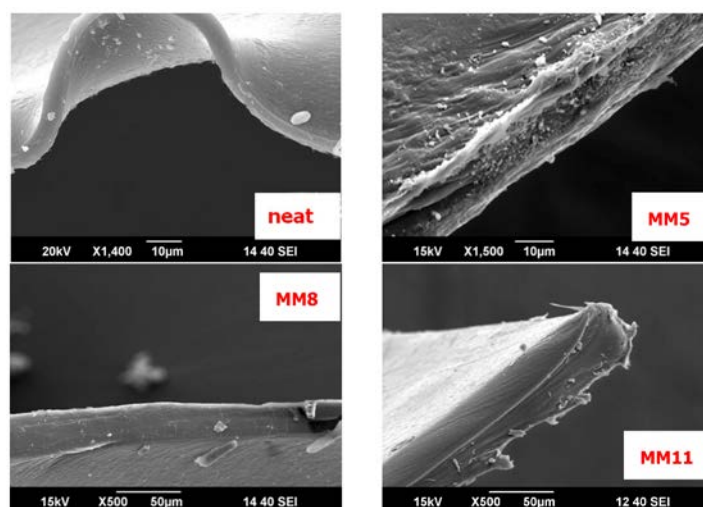


Figure 4. Morphology of dense neat Pebax-1657 and nanocarbon-based Pebax-1657 mixed matrix membranes.

This may be sufficient proof for the homogeneous dispersion of the filler in the polymer matrix, without observable agglomerates or obvious defects in the matrix, indicating the good affinity and adhesion between the polymer and nanofillers. The existence of some white “dots”, especially on the MM5 membrane, can be attributed to dust, which sticks to the surface after membrane cutting preparation with liquid nitrogen as a cooling agent. The membranes are extremely flexible, which becomes obvious in the SEM image of the neat sample (curved membrane).

3.2. FTIR Analysis

The FTIR spectra of the thirteen Pebax-1657-based membranes are shown in Figure 5. All samples exhibit very similar spectra. The peak at 3294 cm^{-1} indicates the presence of N-H amide group [36] and the peaks at 2938 and 2864 cm^{-1} the existence of the aliphatic -C-H groups and the vibrations of the $\delta(\text{C-H})$ and $\nu(\text{C-H})$ [37].

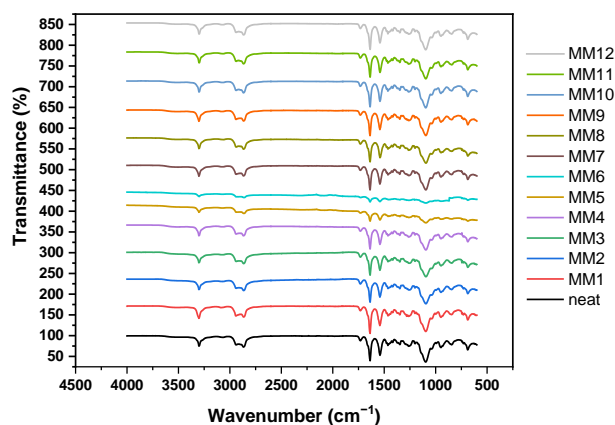


Figure 5. FTIR spectra of the thirteen Pebax-1657 membranes, the neat and the twelve mixed matrix membranes.

The characteristic peaks at 1640 and 1544 cm^{-1} correspond to the hydrogen-bonded amide peak and to the C–O stretching band, respectively. The two characteristic peaks at 1731 and 1099 cm^{-1} correspond to C=O (carbonyl group) and C–O–C (ether group) stretching vibrations in the pure Pebax-1657 structure [38].

3.3. Water Contact Angle Measurements

The water contact angle (WCA) measurements were performed employing a Krüss DSA30S instrument as mentioned. The CA measuring instrument has a range of 180° for surface tensions ranging from 0.01 to 2000 mN/m. A digital image followed by the calculated droplet's contact angle is recorded automatically by the Advance-Krüss software. The instrument provides remarkable reproducibility and high accuracy of measurement [39]. During the measurement, at any equilibrium stage of the drop/surface system, a calculated contact angle is recorded automatically.

The affinity of the membranes' surfaces to water was assessed by the equilibrium contact angle of all studied samples through the contact angle measurements, as shown in Table 2.

Table 2. Water contact angle measurements of the studied flat sheet Pebax-1657-based membranes.

Sample	Neat	MM1	MM2	MM3	MM4	MM5	MM6	MM7	MM8	MM9	MM10	MM11	MM12
Average WCA ($^\circ$)	63.4	83.0	85.0	107.8	76.0	78.0	86.0	69.0	76.6	87.0	68.9	70.5	71.0

with bold are mentioned the higher WCA values of each membrane group.

The presented value of each sample is the average value of five measurements from different spots of the membranes' surfaces. It is obvious that in all cases of mixed matrix membranes, surface hydrophilicity was lower compared to the neat Pebax-1657 membrane. Specifically, the WCA is 63.4° for the neat Pebax-1657 membrane, while for the derived MMMs it fluctuated between 69 and $\sim 108^\circ$. The same behavior was also previously observed for cross-linked Pebax membranes, where higher grade of crosslinking resulted in an analogous increase in surface hydrophobicity [40]. Similarly, this trend has also been presented in a study regarding MWCNTs/Pebax MMMs [41].

In all four groups of mixed matrix membranes (relative to filler's type) a common feature was noticed: An increase in filler concentration leads to a surface hydrophilicity reduction. In particular, the GNP fillers affect more intensely the membranes' hydrophilicity, as these nanomaterials render the property of hydrophobicity sturdier than the MWCNTs. This can be attributed to shape and dimensions (see Section 3.1) of the robust GNPs. The edges of GNP flakes protruding from the surface form a kind of comb at the membrane's surface, which increases its roughness. The existence of the GNPs' edges/wrinkles is probably more in line with a Cassie–Baxter wetting state than a Wenzel state [42], and therefore the surface hydrophilicity decreases. The higher roughness leads to reduction in water wettability. Furthermore, as observed in Table 2, the measured higher WCA values correspond to the modified nanofillers (both cases of MWCNTs and GNPs) and not the raw nanofillers, providing good evidence for their better dispersion and compatibility with the polymeric matrices. The difference of the surface hydrophilicity is apparent in the three selected water contact angle images, which are presented in Figure 6.



Figure 6. Characteristic images of water contact angles on three membrane surfaces.

3.4. Mechanical Properties

The mechanical behavior concerning their Young's modulus, ultimate tensile strength and tensile elongation at fracture of the studied membranes was also investigated [29]. These three characteristic mechanical properties were evaluated from the tensile axial stress–strain curves, and their full calculations have been described in our previous work [43].

In Table 3 and Figure 7, the numerical results of the mechanical tests of all samples are summarized, and the tensile properties of all membranes are depicted. The measurements were performed at ambient humidity of about 50%, whereas the samples were pre-equilibrated at this condition prior to each measurement. By analyzing the data in Table 3, it becomes clear that the values for the twelve MMMs can differ slightly or significantly compared to the “neat” membrane. The characteristic factor, which plays the major role in the determination of the Young's modulus and ultimate tensile strength properties, is the concentration of the nanofiller material. In all four cases of different added nanofiller materials, higher concentration results in higher values of both abovementioned properties. For both properties, the addition of GNPs is more effective than the addition of MWCNTs. The highest values are reached in the cases of oxidized GNPs and plasma-treated MWCNTs and not for the corresponding raw materials. Specifically, for the membranes prepared with oxidized GNPs, the Young's modulus increased up to 3.2 times (MM3) and for membranes with the plasma-treated MWCNTs up to 2.3 times (MM9) compared to the neat polymeric membrane. The observed differences between the mixed matrix membranes with raw and modified nanofillers are explained by the homogeneous and uniform dispersions of the modified GNPs and MWCNTs in the polymeric matrix, leading to stiffness enhancement of the polymer composite.

The Young's modulus value, ~59 MPa, of the neat Pebax-1657 membrane is also reported by Duan et al. [44] in their recent work, where covalent organic frameworks (COFs)-functionalized MMMs were studied concerning CO₂/N₂ performance. Similar to our results is the behavior of the functionalized-GO/Pebax-1657 membranes in the work of Zhang et al. [45], where the addition of functionalized graphene oxide (f-GO) into the Pebax-1657 matrix resulted in higher Young's modulus values, from ~46 MPa for the neat membrane up to 126 MPa for the 0.7 wt.% f-GO/Pebax-1657 sample. In contrast to our results, where the addition of carbon nanofillers led to the increase in the Young's modulus, for the reported addition of COF-5 at concentrations up to 3 wt.%, the Young's modulus was always subordinate to the corresponding neat membrane. This behavior of the Young's modulus detriment has also been observed in another work of Fam et al. [46]. Indeed, for the case of Pebax-1657/ionic liquid (IL) membranes, the initial value of 73.7 MPa was decreased down to 1.2 MPa for the membrane with 80% of IL loading.

Furthermore, the good interfacial adhesion between the polymer and the nanofillers impelled the high toughness of the mixed matrix membranes, and again the ones with embedded treated nanofillers presented better results. Then, the ultimate tensile strengths of MM3 and MM9 membranes were higher than those of the neat membrane by 55.3% and 23.5%, respectively.

On the other hand, the more flexible MWCNT nanofillers enhanced the membranes' elongation at fracture more effectively than the stiffer GNPs nanofillers. An increase up to 64.1% in the elongation at fracture was observed for the 5.3 wt.% plasma-treated MWCNTs fraction (MM9 membrane) compared to the neat polymeric membrane. In contrast, a maximum elongation (210.8%) was achieved for MM10 membrane (0.7 wt.% raw MWCNTs), and a further increase in raw MWCNTs content up to 5.3 wt.% impaired the elongation.

This trend could be explained based on the hypothesis that at high MWCNT loadings, the membranes (MM11 and MM12) become more brittle because of a weaker interfacial binding between polymer and nanofiller and simultaneously a higher restriction of the chains' mobility within the polymer matrix [47,48]; conversely, the stronger interaction between the modified MWCNTs and the polymer matrix caused by the incorporation of functional groups in the nanofiller's structure results in a better outcome.

Table 3. Mechanical properties of the studied flat sheet Pebax-1657-based membranes.

Sample	Filler Material	Filler Fraction (%)	Young's Modulus (MPa)	Ultimate Tensile Strength (MPa)	Elongation at Fracture (%)
neat	—	—	<u>58.7 ± 8.8</u>	<u>7.20 ± 1.35</u>	<u>159.5 ± 21.3</u>
MM1	Oxid. GNPs	0.7	103.6 ± 6.6	8.50 ± 0.44	139.2 ± 8.0
MM2		3.0	137.2 ± 11.9	10.33 ± 0.93	180.2 ± 6.4
MM3		5.3	188.0 ± 8.8	11.18 ± 0.87	150.1 ± 8.0
MM4	Raw GNPs	0.7	117.0 ± 0.7	7.62 ± 0.94	155.5 ± 3.3
MM5		3.0	132.0 ± 2.9	8.86 ± 0.64	137.7 ± 12.9
MM6		5.3	154.8 ± 14.6	10.47 ± 0.93	145.0 ± 11.9
MM7	Plasma MWCNTs	0.7	87.3 ± 0.8	7.46 ± 0.45	226.0 ± 11.2
MM8		3.0	119.3 ± 11.1	8.61 ± 0.37	249.0 ± 7.0
MM9		5.3	135.6 ± 7.1	8.89 ± 0.48	261.7 ± 17.2
MM10	Raw MWCNTs	0.7	87.0 ± 9.5	7.40 ± 0.32	210.8 ± 14.2
MM11		3.0	91.0 ± 8.2	7.53 ± 0.32	164.5 ± 8.7
MM12		5.3	108.4 ± 10.6	7.84 ± 0.35	152.0 ± 10.4

Underline values are referred to the reference material, the neat membrane. Bold values are referred to the higher values of each membrane group.

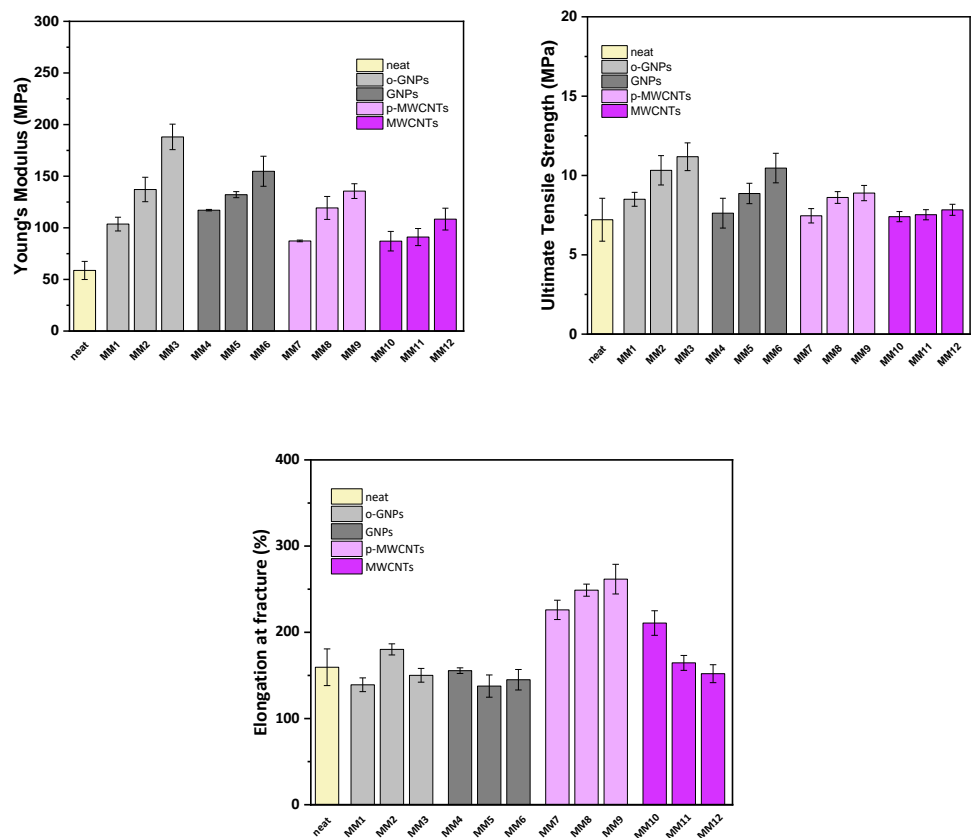


Figure 7. The mechanical behavior (tensile properties) concerning the Young's modulus, ultimate tensile strength and tensile elongation at fracture, as calculated from corresponding stress–strain curves of all studied flat sheet Pebax-1657-based membranes.

The trade-off between ductility and tensile strength has also been reported in literature [49,50]. The rigid agglomerates of MWCNTs in the soft segment of the polymer matrix, forming after an inefficient dispersion, act as stress raisers resulting in premature fracture.

An overall remark is that the type of nanofiller, its modification/treatment (which facilitates its good dispersibility), as well as its weight fraction in the polymer matrix significantly affect the mechanical properties of the prepared mixed matrix membranes.

In order to compare the experimental Young’s modulus and tensile strength of the mixed matrix membranes with theoretical predictions, three (Halpin–Tsai, Ekvall and Whitney–Riley) and two (Halpin–Kardos and Hirsch) well-known models were employed, respectively. Firstly, for the aligned and randomly and unidirectionally distributed filler conditions, the equations of the Halpin–Tsai model are the following [51]:

$$E_c = E_m [3/8 \times (1 + n_L \zeta r \varphi_f / 1 - n_L \varphi_f) + 5/8 \times (1 + 2n_T \varphi_f / 1 - n_T \varphi_f)] \text{ (random)} \quad (2)$$

$$E_c = E_m [(1 + n_L \zeta \varphi_f / 1 - n_L \varphi_f)] \text{ (aligned)} \quad (3)$$

$$n_L = (E_f / E_m - 1) / (E_f / E_m + \zeta) \quad (4)$$

$$n_T = (E_f / E_m - 1) / (E_f / E_m + 2) \quad (5)$$

$$\zeta = k(l_f / t_f) \quad (6)$$

where E_c , E_m and E_f are the Young’s moduli of the composite, the Pebax matrix and the filler (MPa), respectively; φ_f is the volume fraction of the filler in the composite, derived from the equation $\varphi_f = (w_f / \rho_f) / (w_f / \rho_f + (1 - w_f) / \rho_m)$, where w_f is the filler mass fraction and ρ_f and ρ_m the densities of the filler (2.2 and 2.0 g/cm³ for GNPs and MWCNTs, respectively) and the matrix (1.01 g/cm³), respectively; ζ is a parameter regarding the nanofiller’s geometry, distribution and loading with $k = 2/3$ and 2 for GNPs and MWCNTs, respectively; while l_f and t_f refer to the length and thickness/diameter of GNPs/MWCNTs, respectively. These latter parameters were defined by SEM analysis.

According to the Ekvall model, the Young’s modulus is calculated using the following equations [52]:

$$E_c = E_f E'_m / [E'_m \varphi_f + E_f (1 - \nu_m^2) \varphi_m] \quad (7)$$

$$E'_m = E_m / (1 - \nu_m^2) \quad (8)$$

where φ_m is the volume fraction of the matrix in the composite and ν_m is the Poisson’s ratio of the matrix (0.3).

Moreover, for the Whitney–Riley model, the Young’s modulus can be calculated from the following equations [53]:

$$K_f = E_f (1 - \nu_f - 2\nu_f^2) \quad (9)$$

$$K_m = E_m (1 - \nu_m - 2\nu_m^2) \quad (10)$$

$$K_c = [(K_f + G_m)K_m - (K_f - K_m)G_m \varphi_f] / [(K_f + G_m) - (K_f - K_m)\varphi_f] \quad (11)$$

$$E_L = E_m + (E_f - E_m)\varphi_f \quad (12)$$

$$\nu_{yz} = \nu_f \varphi_f + \nu_m (1 - \varphi_f) \quad (13)$$

$$L_m = 1 - \nu_m - 2\nu_m^2 \tag{14}$$

$$L_f = 1 - \nu_f - 2\nu_f^2 \tag{15}$$

$$\nu_c = \nu_m - 2(\nu_m - \nu_f)(1 - \nu_m^2)E_f\varphi_f/E_m(1 - \varphi_f)L_f + [L_m\varphi_f + (1 + \nu_m)]E_f \tag{16}$$

$$E_c = 2K_c(1 - \nu_{yz})E_L/(E_L + 4K_c\nu_c^2) \tag{17}$$

where ν_f is the Poisson’s ratio of the filler (0.22 for GNPs and 0.35 for MWCNTs), and G_m is the shear modulus of the matrix calculated from the equation $G_m = E_m/2(1 + \nu_m)$ (22.6 MPa). For all aforementioned models, the Young’s moduli of matrix (Pebax), GNPs and MWCNTs are 58.7 MPa (from the tensile test), ~1000 GPa and ~600 GPa, respectively.

In Figure 8, the comparison of the theoretical calculations from the three models and the experimental data of the tensile moduli of all MMMs is depicted. For low nanofiller loading (0.7 wt.%) the Halpin–Tsai model for the aligned distributed nanofiller condition of all nanofillers, except raw GNPs, fitted experimental data perfectly. For higher loadings, the Halpin–Tsai model for randomly and unidirectionally distributed nanofillers is most suitable, mainly for the case of modified nanofillers, indicating the quality of a sufficient dispersion and the avoidance of aggregate formation. In general, the other two models, that are based only on Poisson’s ratio, diverge from experimental data to a greater or lesser extent, depending on the type or amount of nanofiller.

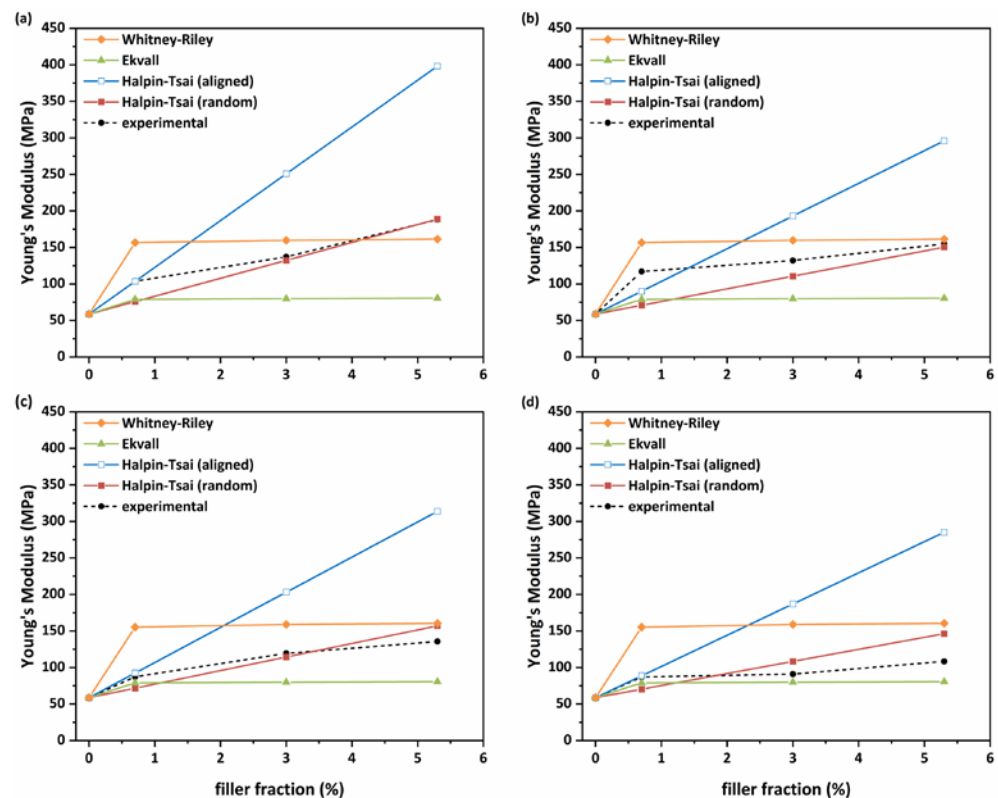


Figure 8. Comparison of the Young’s modulus as theoretically calculated from the Halpin–Tsai, Ekvall and Whitney–Riley models and from the experimental data for MMMs with (a) oxidized GNPs; (b) raw GNPs; (c) plasma-treated MWCNTs and (d) raw MWCNTs.

Similarly, for the theoretical calculations of the composites' ultimate tensile strength, the Halpin–Kardos model is based on the following equations [54]:

$$n = (UTS_f/UTS_m) - 1/(UTS_f/UTS_m) + \zeta \tag{18}$$

$$UTS_c = UTS_m(1 + \zeta n \phi_f / (1 - n \phi_f)) \tag{19}$$

where UTS_f , UTS_m and UTS_m are the ultimate tensile strengths of the filler, matrix and composite (MPa), respectively. Finally, the equation of the Hirsch model is given below [55]:

$$UTS_c = x(UTS_m \phi_m + UTS_f \phi_f) + (1 - x)UTS_f UTS_m / (UTS_m \phi_f + UTS_f \phi_m) \tag{20}$$

where x is a parameter that determines the stress transfer between the matrix and the filler. For both abovementioned models, the tensile strengths of the Pebax matrix, GNPs and MWCNTs are 7.2 MPa (from the tensile test), ~10 GPa and ~20 GPa, respectively.

The overall theoretical calculations are illustrated in Figure 9. As observed, the Hirsch model is apparently more consistent for all types of nanofillers than the Halpin–Kardos model, indicating that parameter x (Equation (20)) is a crucial factor for the prediction of the tensile strength of the composites.

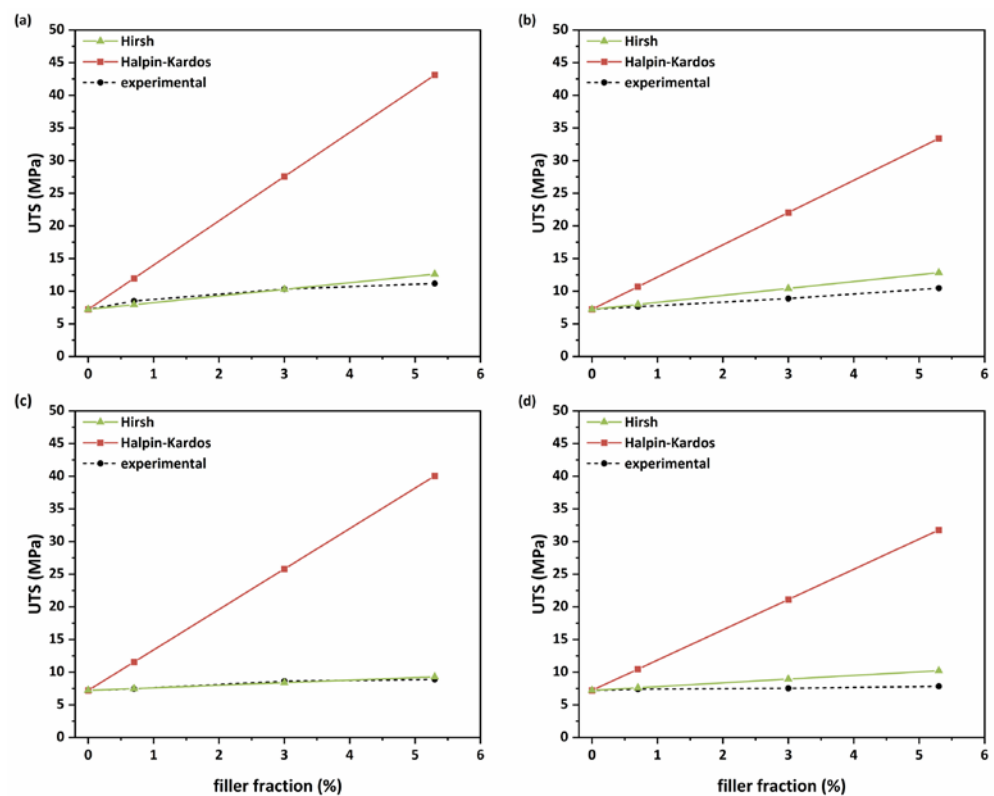


Figure 9. Comparison of the theoretical and experimental tensile strengths of the MMMs with (a) oxidized GNPs; (b) raw GNPs; (c) plasma-treated MWCNTs and (d) raw MWCNTs.

3.5. CO₂/CH₄ Permeability and Selectivity Results

In the present work, the binary CO₂/CH₄ mixture of gases was selected in order to study the membranes' performance based on their permeability and selectivity. Experiments were conducted over a feed pressure range of 1.3 to 5.0 bar at the temperature of 25 °C. The measurements were performed as described in Section 2.4. In Table 4, the CO₂ and CH₄ permeability values and the respective CO₂/CH₄ selectivities for the 10/90 (molar concentrations) CO₂/CH₄ gas mixture are presented at five studied feed pressures of 1.3, 2, 3, 4 and 5 bar.

Table 4. CO₂ permeability (Barrer) and CO₂/CH₄ selectivity values for the thirteen studied membranes for 10% v/v CO₂ in CH₄.

Sample	Filler Material	% Concentr	CO ₂ Permeability (Barrer) at					CO ₂ /CH ₄ Selectivity at				
			1.3	2	3	4	5 (bar)	1.3	2	3	4	5 (bar)
neat	—	—	87.6	80.5	77.4	76.5	80.4	20.2	19.7	19.6	18.4	16.0
MM1	Oxid. GNPs	0.7	76.5	74.8	73.6	73.4	71.4	19.3	19.0	18.4	18.5	18.0
MM2		3.0	127.8	126.8	128.0	126.6	123.1	19.6	19.2	18.9	18.0	17.6
MM3		5.3	95.3	95.6	100.2	101.8	99.9	18.8	18.6	19.1	19.1	18.2
MM4	Raw GNPs	0.7	70.1	71.7	74.0	70.2	67.7	19.0	19.7	19.0	18.4	18.0
MM5		3.0	91.4	91.0	92.4	91.2	91.8	19.2	19.7	19.3	19.2	18.7
MM6		5.3	98.1	96.7	98.4	95.1	90.6	20.2	19.4	19.1	18.5	17.8
MM7	Plasma MWCNTs	0.7	95.6	85.0	82.7	85.9	86.9	19.9	18.4	17.8	18.4	18.0
MM8		3.0	151.6	148.9	145.9	140.0	135.6	18.7	18.9	18.4	17.7	16.8
MM9		5.3	118.4	106.2	107.4	104.5	103.3	20.2	18.1	18.2	17.2	17.0
MM10	Raw MWCNTs	0.7	113.4	108.9	103.8	105.4	98.7	20.5	19.9	19.0	18.9	17.7
MM11		3.0	270.3	285.1	293.8	383.7	375.1	20.5	20.2	21.7	22.7	21.9
MM12		5.3	133.3	95.2	100.5	102.2	102.7	21.0	20.0	20.1	19.7	19.6

Table 4 and Figure 10 exhibit the effect of both GNPs and MWCNTs as four different nanomaterial types for three different filler-loading concentrations. All membranes are selective for CO₂ and present permeability values fluctuating between 67 (MM4 membrane at 5 bar feed pressure) and 384 Barrer (MM11 membrane at 4 bar feed pressure).

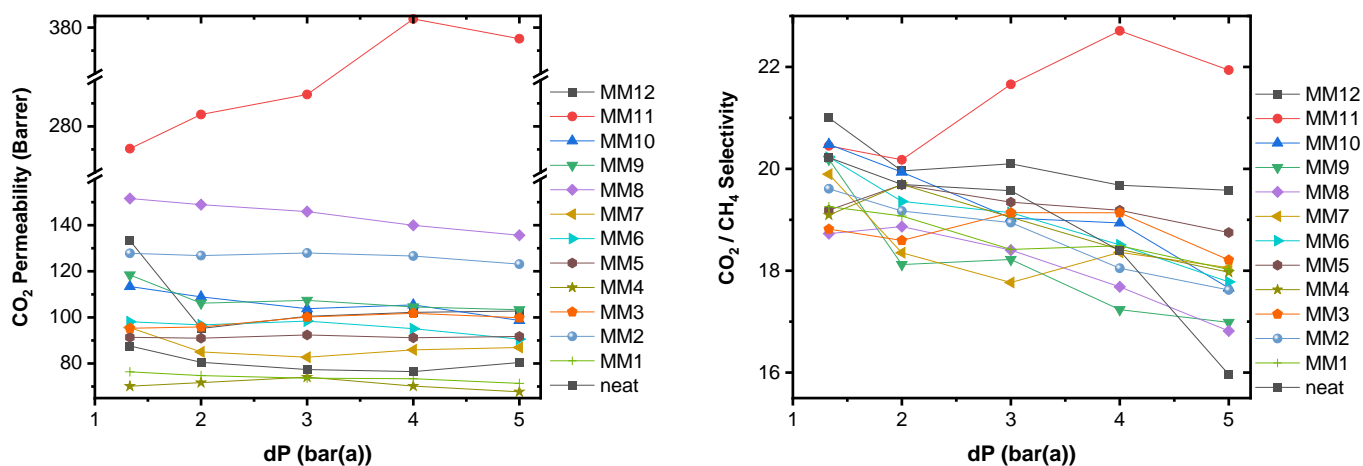


Figure 10. CO₂ permeability (left) and CO₂/CH₄ separation factor (selectivity) (right) versus pressure drop across all studied MMMs for 10% v/v CO₂ in CH₄. Temperature was kept constant at 298 K.

As seen in Table 4, the CO₂ permeability values change in a different manner for the MWCNTs and the GNPs-based MMMs. For the cases of raw and oxidized GNPs (samples MM1 and MM4), a decrease of ~10% in CO₂ permeability is observed for the MMMs loaded with 0.7 wt.% o-GNPs. This can be attributed to the fact that this very low number of GNPs works like a crosslinker material and makes the polymeric matrix less flexible with lower free volume than the neat matrix, resulting in a decrease in gas diffusivity and consequently also gas permeability [56]. By increasing the number of GNPs, the CO₂ permeability also

increases, presenting a maximum value for the concentration of 3 and of 5.3 wt.% in the cases of oxidized and raw GNPs, respectively. This behavior is in correlation with what is reported in literature for Pebax [46,57,58] but also for other polymeric mixed matrix membranes [16,59,60]. Here, it must be noted that the addition of the oxidized GNPs finally provides improved properties and better position in the Robeson plot of selectivity versus permeability, as the selectivity is remaining constant, and simultaneously the CO₂ permeability increases about 46% at 1.3 bar.

On the other hand, in the case of MWCNTs-based MMMs the CO₂ permeability increases even for the very low amount of 0.7 wt.%, whereas GNPs require concentrations above 3 wt.% in order to increase permeability, as mentioned. The smooth one-dimensional nanochannels of the MWCNTs could act as accelerated CO₂ transport pathways through the MMMs. For both raw and plasma-treated carbon nanotubes, and at all feed pressures, higher CO₂ permeability is observed in the case of MMMs with filler concentration of 3 wt.%. Furthermore, the membranes with oxidized GNPs need a concentration of 5.3 wt.% in order to reach MWCNT performance concerning permeability.

Effect of Feed Pressure: All membranes were tested in CO₂/CH₄ (10/90 vol.%) at five different transmembrane pressures, 1.3, 2, 3, 4 and 5 bar. With one exemption (that of the MM11 membrane), for the twelve membranes the influence of feed pressure on CO₂ permeability was negligible. As seen in Table 4 and Figure 10, only small fluctuations, of about ±2–7%, in CO₂ permeability were observed as pressure rose from 1.3 to 5 bar. However, for the MM11 membrane, the effect of feed pressure on CO₂ permeability was positive, with an increase from 270 Barrer at feed pressure 1.3 bar to 384 Barrer at feed pressure of 4 bar.

On the contrary, the effect of pressure on CO₂/CH₄ selectivity is negative with a slight decrease compared to the value of the neat membrane. The only exception to this trend was observed for the M11 membrane (see Figure 10). At this point, irrespective of their concentration, nanofillers retain the selectivity of the neat membrane above 4 bar, withstanding membrane compaction. Overall, MMMs exhibited enhanced gas permeabilities with up to fivefold values without sacrificing selectivity compared to the neat polymeric membrane.

4. Conclusions and Outlook

Pebax-1657 mixed matrix flat sheet membranes were prepared following the solution casting/solvent evaporation technique, characterized and tested concerning their CO₂/CH₄ separation performance. Two types of carbon nanofillers were used, namely multi-walled carbon nanotubes and graphene nanoplatelets, both as raw materials but also after plasma treatment modification and oxidation process, respectively. In both cases, the modified nanomaterials (the oxidized GNPs and the plasma-treated MWCNTs) had a stronger reduction effect on water wettability of the prepared MMMs. The addition of these carbon-based nanomaterials resulted in membranes with improved mechanical properties and higher CO₂ permeability, while selectivity was maintained at the level of the neat membrane. The polar groups of modified nanofillers form hydrogen bonds with the polymeric chains of Pebax, and hydrogen bonding interactions between nanofillers and Pebax are developed, resulting in the polymer chain packing disturbance and increase in free volume (voids) for the CO₂ and CH₄ molecules penetration and consequently the increase in gas diffusion (permeability). Furthermore, the functional groups on the surface of nanofillers may interact with gases (e.g., CO₂) and increase the solubility in the MMMs, as the CO₂ gas transition through the MMMs is facilitated. Improved withstanding of membrane compaction was an additional benefit of all examined nanofillers. The CO₂/CH₄ separation factor of the tested mixture of 10/90 (mole fraction) fluctuated between 16 and 21, with the higher values being observed at the lowest transmembrane pressure of 1.3 bar. A general conclusion is that MMMs exhibited enhanced gas permeabilities up to fivefold values (~384 Barrer for MM11) without sacrificing the gas selectivity in comparison with the neat membrane.

Author Contributions: Conceptualization, A.N.V., G.V.T. and E.P.F.; methodology, G.V.T., D.S.K., M.B., A.A.S. and E.P.F.; validation, D.S.K., M.B. and E.P.F.; formal analysis, A.N.V., G.V.T. and D.S.K.; investigation, D.S.K., M.B., A.A.S. and E.P.F.; resources, A.A.S. and E.P.F.; data curation, A.N.V. and G.V.T.; writing—original draft preparation, G.V.T. and E.P.F.; writing—review and editing, G.V.T., D.S.K. and E.P.F.; supervision, G.V.T., D.S.K. and E.P.F.; project administration, E.P.F.; funding acquisition, A.A.S. and E.P.F. All authors have read and agreed to the published version of the manuscript.

Funding: This research was funded. The authors would like to acknowledge the support of the project entitled “CO₂ separation by using mixed matrix, based on nano-carbon materials membranes (GG-CO₂)”, implemented under the “Action for the Strategic Cooperation between Greek and German Academia and Industry”, funded by the Operational Programme “Competitiveness, Entrepreneurship and Innovation” (NSRF 2014–2020), funded by German Ministry BMBF (03XP0153A) and co-financed by Greece and the European Union (European Regional Development Fund).

Institutional Review Board Statement: Not applicable.

Informed Consent Statement: Not applicable.

Data Availability Statement: Not applicable.

Acknowledgments: The authors would like to acknowledge the support of the project entitled “CO₂ separation by using mixed matrix, based on nano-carbon materials membranes (GG-CO₂)”, implemented under the “Action for the Strategic Cooperation between Greek and German Academia and Industry”, funded by the Operational Programme “Competitiveness, Entrepreneurship and Innovation” (NSRF 2014–2020) and co-financed by Greece and the European Union (European Regional Development Fund). The authors would also like to thank S. Forero and Jan Benra (FutureCarbon GmbH) for providing the carbon nanomaterials and R. Kosheleva (Hephaestus Lab, International Hellenic University) for her valuable support in performing FTIR and SEM experiments.

Conflicts of Interest: The authors declare no conflict of interest.

References

1. Favvas, E.P.; Katsaros, F.K.; Papageorgiou, S.K.; Sapalidis, A.A.; Mitropoulos, A.C. A Review of the Latest Development of Polyimide based Membranes for CO₂ Separations. *React. Funct. Polym.* **2017**, *120*, 104–130. [\[CrossRef\]](#)
2. Azizi, N.; Mohammadi, T.; Behbahani, R.M. Synthesis of a new nanocomposite membrane (PEBAX-1074/PEG-400/TiO₂) in order to separate CO₂ from CH₄. *J. Nat. Gas Sci. Eng.* **2017**, *37*, 39–51. [\[CrossRef\]](#)
3. Robeson, L.M. The upper bound revisited. *J. Membr. Sci.* **2007**, *320*, 390–400. [\[CrossRef\]](#)
4. Yeo, Z.Y.; Chew, T.L.; Zhu, P.W.; Mohamed, A.R.; Chai, S.P. Conventional Processes and Membrane Technology for Carbon Dioxide Removal from Natural Gas: A Review. *J. Nat. Gas Chem.* **2012**, *32*, 282–298. [\[CrossRef\]](#)
5. Salehi, E.; Heidary, F.; Daraei, P.; Keyhani, M.; Behjomanesh, M. Carbon nanostructures for advanced nanocomposite mixed matrix membranes: A comprehensive overview. *Rev. Chem. Eng.* **2020**, *36*, 723–748. [\[CrossRef\]](#)
6. Mannan, H.A.; Mukhtar, H.; Murugesan, T.; Nasir, R.; Mohshim, D.F.; Mushtaq, A. Recent Applications of Polymer Blends in Gas Separation Membranes. *Chem. Eng. Technol.* **2013**, *36*, 1838–1846. [\[CrossRef\]](#)
7. Xu, W.; Zhao, Y.; Yuan, Z.; Li, X.; Zhang, H.; Vankelecom, I.F.J. Highly Stable Anion Exchange Membranes with Internal Cross-Linking Networks. *Adv. Funct. Mater.* **2015**, *25*, 2583–2589. [\[CrossRef\]](#)
8. Amirilargani, M.; Sadrzadeh, M.; Sudhölter, E.J.R.; de Smet, L.C.P.M. Surface modification methods of organic solvent nanofiltration membranes. *Chem. Eng. J.* **2016**, *289*, 562–582. [\[CrossRef\]](#)
9. Ang, M.B.M.Y.; Tang, C.-L.; De Guzman, M.R.; Maganto, H.L.C.; Caparanga, A.R.; Huang, S.-H.; Tsai, H.-A.; Hu, C.-C.; Lee, K.-R.; Lai, J.-Y. Improved performance of thin-film nanofiltration membranes fabricated with the intervention of surfactants having different structures for water treatment. *Desalination* **2020**, *481*, 114352. [\[CrossRef\]](#)
10. Xiang, J.; Xie, Z.; Hoang, M.; Zhang, K. Effect of amine salt surfactants on the performance of thin film composite poly(piperazine-amide) nanofiltration membranes. *Desalination* **2013**, *315*, 156–163. [\[CrossRef\]](#)
11. Agboola, O.; Sadiku, E.R.; Mokrani, T. Nanomembrane materials based on polymer blends. In *Design and Applications of Nanostructured Polymer Blends and Nanocomposite Systems*; Thomas, S., Shanks, R., Chandrasekharakurup, S., Eds.; Elsevier: Oxford, UK, 2016; pp. 101–123.
12. Yao, M.; Woo, Y.C.; Tijing, L.D.; Cesarini, C.; Shon, H.K. Improving Nanofiber Membrane Characteristics and Membrane Distillation Performance of Heat-Pressed Membranes via Annealing Post-Treatment. *Appl. Sci.* **2017**, *7*, 78. [\[CrossRef\]](#)
13. Salehi, E.; Madaeni, S.S.; Heidary, F. Dynamic adsorption of Ni(II) and Cd(II) ions from water using 8-hydroxyquinoline ligand immobilized PVDF membrane: Isotherms, thermodynamics and kinetics. *Sep. Purif. Technol.* **2012**, *94*, 1–8. [\[CrossRef\]](#)
14. Dechnik, J.; Gascon, J.; Doonan, C.J.; Janiak, C.; Sumbly, C.J. Mixed-Matrix Membranes. *Angew. Chem. Int.* **2017**, *56*, 9292–9310. [\[CrossRef\]](#) [\[PubMed\]](#)

15. Favvas, E.P.; Stefanopoulos, K.L.; Nolan, J.W.; Papageorgiou, S.K.; Mitropoulos, A.C.; Lairez, D. Mixed matrix hollow fiber membranes with enhanced gas permeation properties. *Sep. Purif. Technol.* **2014**, *132*, 336–345. [[CrossRef](#)]
16. Favvas, E.P.; Nitodas, S.F.; Stefanopoulos, A.; Stefanopoulos, K.L.; Papageorgiou, S.K.; Mitropoulos, A.C. High Purity Multi-Walled Carbon Nanotubes: Preparation, Characterization and Performance as Filler Materials in co-polyimide Hollow Fiber Membranes. *Sep. Purif. Technol.* **2014**, *122*, 262–269. [[CrossRef](#)]
17. Moore, T.T.; Mahajan, R.; Vu, D.Q.; Koros, W.J. Hybrid membrane materials comprising organic polymers with rigid dispersed phases. *AIChE J.* **2004**, *50*, 311–321. [[CrossRef](#)]
18. Kamble, A.R.; Patel, C.M.; Murthy, Z.V.P. A review on the recent advances in mixed matrix membranes for gas separation processes. *Renew. Sustain. Energy Rev.* **2021**, *145*, 111062. [[CrossRef](#)]
19. Najari, S.; Saeidi, S.; Gallucci, F.; Drioli, E. Mixed matrix membranes for hydrocarbons separation and recovery: A critical review. *Rev. Chem. Eng.* **2021**, *37*, 363–406. [[CrossRef](#)]
20. Krokidas, P.; Spera, M.B.M.; Boutsika, L.G.; Bratsos, I.; Charalambopoulou, G.; Economou, I.G.; Steriotis, T. Nanoengineered ZIF fillers for mixed matrix membranes with enhanced CO₂/CH₄ selectivity. *Separ. Purif. Technol.* **2023**, *307*, 122737. [[CrossRef](#)]
21. Farashi, Z.; Azizi, S.; Arzhandi, M.R.-D.; Noroozi, Z.; Azizi, N. Improving CO₂/CH₄ separation efficiency of Pebax-1657 membrane by adding Al₂O₃ nanoparticles in its matrix. *J. Nat. Gas Sci. Eng.* **2019**, *72*, 103019. [[CrossRef](#)]
22. Embaye, A.S.; Martínez-Izquierdo, L.; Malankowska, M.; Téllez, C.; Coronas, J. Poly(ether-block-amide) Copolymer Membranes in CO₂ Separation Applications. *Energy Fuels* **2021**, *35*, 17085–17102. [[CrossRef](#)]
23. Liu, Y.; Yu, S.; Wu, H.; Li, Y.; Wang, S.; Tian, Z.; Jiang, Z. High permeability hydrogel membranes of chitosan/poly ether-block-amide blends for CO₂ separation. *J. Membr. Sci.* **2014**, *469*, 198–208. [[CrossRef](#)]
24. Estahbanati, E.G.; Omidkhah, M.; Amooghin, A.E. Preparation and characterization of novel Ionic liquid/Pebax membranes for efficient CO₂/light gases separation. *J. Ind. Eng. Chem.* **2017**, *51*, 77–89. [[CrossRef](#)]
25. Zhang, Y.; Shen, Y.; Hou, J.; Zhang, Y.; Fam, W.; Liu, J.; Bennett, T.D.; Chen, V. Ultrasensitive Pebax Membranes Enabled by Templated Microphase Separation. *ACS Appl. Mater. Interfaces* **2018**, *10*, 20006–20013. [[CrossRef](#)] [[PubMed](#)]
26. Dong, G.; Hou, J.; Wang, J.; Zhang, Y.; Chen, V.; Liu, J. Enhanced CO₂/N₂ separation by porous reduced graphene oxide/Pebax mixed matrix membranes. *J. Membr. Sci.* **2016**, *520*, 860–868. [[CrossRef](#)]
27. Huang, T.-C.; Liu, Y.-C.; Lin, G.-S.; Lin, C.-H.; Liu, W.-R.; Tung, K.-L. Fabrication of pebax-1657-based mixed-matrix membranes incorporating N-doped few-layer graphene for carbon dioxide capture enhancement. *J. Membr. Sci.* **2020**, *602*, 117946. [[CrossRef](#)]
28. Iqbal, A.K.M.A.; Sakib, N.; Iqbal, A.K.M.P.; Nuruzzaman, D.M. Graphene-based nanocomposites and their fabrication, mechanical properties and applications. *Materialia* **2020**, *12*, 100815. [[CrossRef](#)]
29. Sapalidis, A.A.; Katsaros, F.K.; Steriotis, T.A.; Kanellopoulos, N.K. Properties of Poly(vinyl alcohol)—Bentonite Clay Nanocomposite Films in Relation to Polymer–Clay Interactions. *J. Appl. Polym. Sci.* **2012**, *123*, 1812–1821. [[CrossRef](#)]
30. Stoitsas, K.A.; Gotzias, A.; Kikkinides, E.S.; Steriotis, T.A.; Kanellopoulos, N.K.; Stoukides, M.; Zaspalis, V.T. Porous ceramic membranes for propane–propylene separation via the p-complexation mechanism: Unsupported systems. *Microporous Mesoporous Mater.* **2005**, *78*, 235–243. [[CrossRef](#)]
31. Favvas, E.P.; Heliopoulos, N.S.; Papageorgiou, S.K.; Mitropoulos, A.C.; Kapantaidakis, G.C.; Kanellopoulos, N.K. Helium and hydrogen selective carbon hollow fiber membranes: The effect of pyrolysis isothermal time. *Sep. Purif. Technol.* **2015**, *142*, 176–181. [[CrossRef](#)]
32. Esser, T.; Wolf, T.; Schubert, T.; Benra, J.; Forero, S.; Maistros, G.; Barbe, S.; Theodorakopoulos, G.V.; Karousos, D.S.; Sapalidis, A.A.; et al. CO₂/CH₄ and He/N₂ separation properties and water permeability valuation of mixed matrix MWCNTs-based cellulose acetate flat sheet membranes: A study of the optimization of the filler material dispersion method. *Nanomaterials* **2021**, *11*, 280. [[CrossRef](#)] [[PubMed](#)]
33. Favvas, E.P.; Papageorgiou, S.K.; Stefanopoulos, K.L.; Nolan, J.W.; Mitropoulos, A.C. Effect of air gap on gas permeance/selectivity performance of BTDA-TDI/MDI co-polyimide hollow fiber membranes. *J. Appl. Polym. Sci.* **2013**, *130*, 4490–4499.
34. Pereira, C.M.C.; Nóvoa, P.; Martins, M.; Forero, S.; Hepp, F. Characterization of carbon nanotube 3D-structures infused with low viscosity epoxy resin system. *Compos. Struct.* **2010**, *92*, 2252–2257. [[CrossRef](#)]
35. Hammerstein, R.; Schubert, T.; Braun, G.; Wolf, T.; Barbe, S.; Quade, A.; Foest, R.; Karousos, D.S.; Favvas, E.P. The optimization of dispersion and application techniques for nanocarbon-doped mixed matrix gas separation membranes. *Membranes* **2022**, *12*, 87. [[CrossRef](#)]
36. Murali, R.S.; Sridhar, S.; Sankarshana, T.; Ravikumar, Y.V.L. Gas Permeation behavior of Pebax-1657 nanocomposite membrane incorporated with multiwalled carbon nanotubes. *Ind. Eng. Chem. Res.* **2010**, *49*, 6530–6538. [[CrossRef](#)]
37. Habib, N.; Durak, O.; Zeeshan, M.; Uzun, A.; Keskin, S. A novel IL/MOF/polymer mixed matrix membrane having superior CO₂/N₂ selectivity. *J. Membr. Sci.* **2022**, *658*, 120712. [[CrossRef](#)]
38. Wang, S.; Liu, Y.; Huang, S.; Wu, H.; Li, Y.; Tian, Z.; Jiang, Z. Pebax–PEG–MWCNT hybrid membranes with enhanced CO₂ capture properties. *J. Membr. Sci.* **2014**, *460*, 62–70. [[CrossRef](#)]
39. Arkas, M.; Favvas, E.P.; Giannakopoulos, K.; Mouti, N.; Karakasliotis, I.; Vardavoulias, M.; Arvanitopoulou, M.; Athanasiou, A.; Kythreoti, G.; Soto, S.M. Hydrophilic antimicrobial coatings for medical leathers from silica-dendritic polymer-silver nanoparticle composite xerogels. *Textiles* **2022**, *2*, 464–485. [[CrossRef](#)]
40. Aburabie, J.; Peinemann, K.-V. Crosslinked poly(ether block amide) composite membranes for organic solvent nanofiltration applications. *J. Membr. Sci.* **2017**, *523*, 264–272. [[CrossRef](#)]

41. Ge, C.; Wang, G.; Zhao, J.; Zhao, G. Poly(ether-block-amide) membrane with deformability and adjustable surface hydrophilicity for water purification. *Polym. Eng. Sci.* **2021**, *61*, 2137–2146. [[CrossRef](#)]
42. Mitropoulos, A.C.; Stefanopoulos, K.L.; Favvas, E.P.; Vansant, E.F.; Hankins, N. On the Formation of Nanobubbles in Vycor Porous Glass During Desorption of Halogenated Hydrocarbons. *Sci. Rep.* **2015**, *5*, 10943. [[CrossRef](#)] [[PubMed](#)]
43. Theodorakopoulos, G.V.; Karousos, D.S.; Mansouris, K.G.; Sapolidis, A.A.; Kouvelos, E.P.; Favvas, E.P. Graphene nanoplatelets based polyimide/Pebax dual-layer mixed matrix hollow fiber membranes for CO₂/CH₄ and He/N₂ separations. *Int. J. Greenh. Gas Control.* **2022**, *114*, 103588. [[CrossRef](#)]
44. Duan, K.; Wang, J.; Zhang, Y.; Liu, J. Covalent organic frameworks (COFs) functionalized mixed matrix membrane for effective CO₂/N₂ separation. *J. Membr. Sci.* **2019**, *572*, 588–595. [[CrossRef](#)]
45. Zhang, J.; Xin, Q.; Li, X.; Yun, M.; Xu, R.; Wang, S.; Li, Y.; Lin, L.; Ding, X.; Ye, H.; et al. Mixed matrix membranes comprising aminosilane-functionalized graphene oxide for enhanced CO₂ separation. *J. Membr. Sci.* **2019**, *570*, 343–354. [[CrossRef](#)]
46. Fam, W.; Mansouri, J.; Li, H.; Chen, V. Improving CO₂ separation performance of thin film composite hollow fiber with Pebax[®]1657/ionic liquid gel membranes. *J. Membr. Sci.* **2017**, *537*, 54–68. [[CrossRef](#)]
47. Prolongo, S.G.; Moriche, R.; Jiménez-Suárez, A.; Sánchez, M.; Ureña, A. Advantages and disadvantages of the addition of graphene nanoplatelets to epoxy resins. *Eur. Polym. J.* **2014**, *61*, 206–214. [[CrossRef](#)]
48. Al-Saleh, M.A.; Yussuf, A.A.; Al-Enezi, S.; Kazemi, R.; Wahit, M.U.; Al-Shammari, T.; Al-Banna, A. Polypropylene/graphene nanocomposites: Effects of GNP loading and compatibilizers on the mechanical and thermal properties. *Materials* **2019**, *12*, 3924. [[CrossRef](#)]
49. Chatterjee, S.; Nüesch, F.A.; Chu, B.T.T. Comparing carbon nanotubes and graphene nanoplatelets as reinforcements in polyamide 12 composites. *Nanotechnology* **2011**, *22*, 275714. [[CrossRef](#)]
50. Alexopoulos, N.D.; Favvas, E.P.; Vairis, A.; Mitropoulos, A.C. MWCNTs/resin nanocomposites: Structural, thermal, mechanical and dielectric investigation. *J. Eng. Sci. Technol. Rev.* **2015**, *8*, 7–14. [[CrossRef](#)]
51. Wang, R.; Aakyir, M.; Qiu, A.; Oh, J.-A.; Adu, P.; Meng, Q.; Ma, J. Surface-tunable, electrically conductive and inexpensive graphene platelets and their hydrophilic polymer nanocomposites. *Polymer* **2020**, *205*, 122851. [[CrossRef](#)]
52. Ekvall, J.C. Structural behaviour of monofilament composites. In Proceedings of the AIAA 6th Structures and Materials Conference, Atlanta, GA, USA, 1–3 February 1965; AIAA: New York, NY, USA, 1965.
53. Whitney, J.M.; Riley, M.B. Elastic properties of fiber reinforced composite materials. *AIAA J.* **1966**, *4*, 1537–1542. [[CrossRef](#)]
54. Halpin, J.C.; Kardos, J.L. The Halpin-Tsai equations: A review. *Polym. Eng. Sci.* **1976**, *16*, 344–352.
55. Venkateshwaran, N.; Elayaperumal, A. Modeling and evaluation of tensile properties of randomly oriented banana/epoxy composite. *J. Reinf. Plast. Compos.* **2011**, *30*, 1957–1967. [[CrossRef](#)]
56. Melicchio, A.; Favvas, E.P. Preparation and characterization of graphene oxide as a candidate filler material for the preparation of mixed matrix polyimide membranes. *Surf. Coat. Technol.* **2018**, *349*, 1058–1068. [[CrossRef](#)]
57. Zhao, D.; Ren, J.; Li, H.; Li, X.; Deng, M. Gas separation properties of poly(amide-6-b-ethylene oxide)/amino modified multi-walled carbon nanotubes mixed matrix membranes. *J. Membr. Sci.* **2014**, *467*, 41–47. [[CrossRef](#)]
58. Pishva, S.; Hassanajili, S. Investigation on effect of ionic liquid on CO₂ separation performance and properties of novel co-casted dual-layer PEBAX-ionic liquid/PES composite membrane. *J. Ind. Eng. Chem.* **2022**, *107*, 180–196. [[CrossRef](#)]
59. Sapolidis, A.A.; Karantzis, P.I.; Vairis, A.; Barbe, S.; Nitodas, S.; Favvas, E.P. A study of reinforcement effect by MWCNTs into BTDA-TDI/MDI (P84) polyimide flat sheet membranes. *Polymers* **2020**, *12*, 1381. [[CrossRef](#)]
60. Bernardo, P.; Clarizia, G. Enhancing Gas Permeation Properties of Pebax[®] 1657 Membranes via polysorbate nonionic surfactants doping. *Polymers* **2020**, *12*, 253. [[CrossRef](#)]

Disclaimer/Publisher’s Note: The statements, opinions and data contained in all publications are solely those of the individual author(s) and contributor(s) and not of MDPI and/or the editor(s). MDPI and/or the editor(s) disclaim responsibility for any injury to people or property resulting from any ideas, methods, instructions or products referred to in the content.